White matter degeneration in aging, a longitudinal diffusion MRI analysis

Marius de Groot, Lotte G.M. Cremers, M. Arfan Ikram, Albert Hofman,Gabriel P. Krestin, Aad van der Lugt, Wiro J. Niessen, Meike W. Vernooij

Radiology 2016

ABSTRACT

Purpose To determine longitudinally the rate of change in diffusion tensor imaging (DTI) parameters of white matter microstructure in aging, and to investigate whether cardiovascular risk factors influence this longitudinal change.

Materials and methods A dedicated ethics committee overseen by national government approved this prospective, population-based cohort study and all participants gave written informed consent. Non-demented, community-dwelling participants were scanned using a research-dedicated 1.5T MRI scanner on two separate visits, on average 2.0 years apart. Out of 810 persons who were eligible for scanning at baseline, longitudinal imaging was available for 501 persons, mean age 69.9 years (range 64.1-91.1 years). Changes of normal-appearing white matter DTI characteristics in the tract-centers were analyzed first globally to investigate diffuse patterns of change, then locally using voxelwise multi-linear regressions. We assessed the influence of cardiovascular risk factors by treating them as additional determinants in both analyses.

Results Over the 2.0 year follow-up interval, global fractional anisotropy (FA) decreased by 0.0042 ($p<10^{-6}$), while mean diffusivity (MD) increased by 8.1 x 10^{-6}mm^2/s ($p<10^{-6}$). Voxelwise analysis of the brain white matter skeleton showed an average decrease of FA of 0.0082 (p_{mean}= 0.002) in 57% of skeleton voxels. The sensorimotor pathway, however, demonstrated an increase of FA of 0.0078 (p_{mean}= 0.009). MD increased on average 10.8 x 10^{-6}mm^2/s ($p_{mean}< 0.001$), in 79% of white matter skeleton voxels. Additionally, we found that white matter degeneration was more pronounced in higher age. Cardiovascular risk factors were generally not associated with longitudinal changes in white matter microstructure.

Conclusions Longitudinal diffusion analysis indicates widespread microstructural deterioration of the normal-appearing white matter in normal aging, with relative sparing of sensorimotor fibers.

INTRODUCTION

It has been recognized that not only grey matter loss, but also white matter deterioration plays an important role in brain aging and cognitive decline[1] and a vascular etiological pathway is often hypothesized.[2] Diffusion tensor imaging (DTI) is a non-invasive magnetic resonance imaging (MRI) technique that measures diffusion of water, and that can quantify subtle changes of white matter tissue organization not visible on structural MRI. DTI provides multiple descriptors of diffusion, with fractional anisotropy (FA) and mean diffusivity (MD) most widely used. FA describes the directionality of diffusion and a lower value typically reflects reduced microstructural organization in regions where white matter fibers are aligned. MD represents the overall magnitude of water diffusion and generally a higher value reflects reduced microstructural organization.[3] Reduced microstructural white matter organization possibly impedes communication within and between neurocognitive networks, which might result in cognitive impairment.[4] In order to identify persons at a higher risk of neurodegenerative disease, it is important to quantify changes in brain tissue in an early stage.[5] This however also requires characterization of baseline age-related changes. The quantitative nature makes DTI very suitable for longitudinal analyses, which are likely to be more sensitive in the early detection of changes in white matter microstructure. However, longitudinal data are still scarce and studies are mostly performed in small sample sizes and in patients with cognitive impairment or Alzheimer's disease.[6-9] The sparse longitudinal findings in 'normal' aging did however corroborate evidence from cross-sectional studies, which showed that during normal aging white matter demonstrates lower FA, with less uniform observations for regions with crossing fibers, combined with higher MD[6-11], and that those aging effects differ across brain regions.[8,9,12,13] Yet, these results need to be corroborated in larger longitudinal studies.

In the current study, we therefore aimed to longitudinally determine the rate of change in DTI parameters of white matter microstructure in aging, and to investigate whether cardiovascular risk factors influence this longitudinal change.[14-15]

METHODS

Study population

This study is based on participants from the Rotterdam Study, a prospective, population-based cohort study that investigates causes and consequences of age-related diseases.[16] The original study population consisted of 7983 participants aged 55 years and older within Ommoord, a suburb of Rotterdam. In 2000, the cohort was expanded with 3011 persons (≥55 years) living in the study area and not included before (16). Since 2005, brain MRI is incorporated in the core protocol of the study. In 2005 and 2006, a group of 1073 participants was randomly selected from the cohort expansion to participate in the Rotterdam Scan Study.[17] Participants were scanned three times, in 2005-2006, 2008-2009 and in 2011-2012. The latter two time points included an upgraded DTI acquisition that was used for the current analysis, defining the 2008-2009 scan as baseline, and the 2011-2012 scan as follow-up. We excluded individuals who (at either time point) were demented or had MRI contraindications (including claustrophobia). For the 2008-2009 scan, 899 out of the original 1073 persons could be invited, of whom 810 were eligible and 741 participated. At follow up in 2011-2012, 649 out of 741 were re-invited, 625 were eligible and 548 participated. We excluded participants with an incomplete acquisition (n=5), persons with MRI-defined cortical infarcts (n=20), and scans with artifacts hampering automated processing (n=22), resulting in 501 participants with longitudinal DTI data available for analysis. The Rotterdam Population Study Act Rotterdam Study, executed by the Ministry of Health, Welfare and Sports of the Netherlands. Written informed consent was obtained from all participants.

MRI acquisition

Multi-sequence MRI was performed with identical scan parameter settings at both time points on a 1.5T scanner (GE Signa Excite) dedicated to the study and maintained without major hardware or software updates.[17] In short, imaging included a T1-weighted 3D Fast RF Spoiled Gradient Recalled Acquisition in Steady State with an inversion recovery pre-pulse (FASTSPGR-IR) sequence, a proton density (PD) weighted sequence, and a T2-weighted fluid-attenuated inversion recovery (FLAIR) sequence.[17] For DTI, we performed a single shot, diffusion-weighted spin echo echo-planar imaging sequence (repetition time=8575 ms, echo time=82.6 ms, field-of-view=210×210 mm, matrix=96×64 (phase encoding) (zero-padded in k-space to 256×256) slice thickness=3.5 mm, 35 contig uous slices). Maximum b-value was 1000 s/mm^2 in 25 non-collinear directions; three volumes were acquired without diffusion weighting (b-value=0 s/mm^2).

Tissue segmentation

Baseline scans were segmented into grey matter, white matter, cerebrospinal fluid (CSF) and background tissue using an automatic segmentation method.[18] An automatic post-processing step distinguished normal-appearing white matter from white matter lesions (WML), based on the FLAIR image and the tissue segmentation.[19] Intracranial volume (ICV) (excluding the cerebellum with surrounding CSF) was estimated by summing total grey and white matter, and CSF volumes. The WML segmentation was mapped into DTI image space using boundary based registration[20] performed on the white matter segmentation, the b=0 and T1-weighted image.

DTI processing

Diffusion data was pre-processed using a standardized processing pipeline.[21] In short, DTI data was corrected for subject motion and eddy currents by affine co-registration of the diffusion-weighted volumes to the b=0 volumes, including correction of gradient vector directions. Diffusion tensors were estimated using a non-linear Levenberg-Marquardt estimator, available in ExploreDTI.[22] FA and MD, measures of tissue microstructure, were computed from the tensor images. Tensor fits were inspected for artifacts by reviewing axial slices of the FA images (MG, researcher with 5 years experience in diffusion image analysis and LGMC, radiologist in training with 2 years experience in diffusion image analysis).

Image registration

Intra-subject correspondence (between the two time points), and correspondence between subjects was achieved by image registration. Improved tract-based spatial statistics (TBSS) was used with optimized high degree-of-freedom registration in lieu of the two stage registration-projection approach implemented in the original TBSS method.[23,24] All registrations were inspected by reviewing axial compilations of superpositioned moving and target images (MG and LGMC). Following the registration, individual change in diffusion measures could be computed in standard space (MNI152, as provided with the FSL software[25]) by subtracting baseline from follow-up images.
A study specific white matter skeleton was constructed using the TBSS skeletonization procedure on the average FA image composed of all subject images at both time points combined in standard space; thresholding the FA skeleton at 0.25. This skeleton was then used to mask the difference images for longitudinal statistical analysis.

Assessment of risk factors

The following cardiovascular risk factors were assessed based on information derived from home interviews and physical examinations[16], at a single time point prior to baseline MRI-scanning. Blood pressure was measured twice in sitting position using a

random-zero sphygmomanometer. Use of anti-hypertensive drugs was recorded. Diabetes mellitus status was determined on fasting serum glucose level (>= 7.0 mmol/l), non-fasting serum glucose level (>=11.1 mmol/l) or the use of anti-diabetic medication. Smoking was assessed by interview and coded as never, former and current. Total and high-density lipoprotein (HDL) cholesterol were determined in blood serum, while recording the use of lipid lowering medication. *Apolipoprotein E (APOE)*-ε4 allele carriership was assessed on coded genomic DNA samples. Assessment of risk factors predated the baseline MRI on average 3 years.

Statistical analysis

Changes in diffusion characteristics were investigated in two ways: globally and locally, both using the skeletonized difference measurements. For the global analysis, we investigated the average change in FA and MD over the entire skeleton per subject, excluding voxels labeled as WML in the baseline scan. We assessed whether there was a global change in diffusion measures with multiple linear regression using three models. In model 1, we adjusted for age, sex, scan-interval and ICV. We additionally considered alternatives to model 1 in which we corrected for individual measures of white matter macrostructure: white matter atrophy (using normal-appearing white matter volume) or WML load (natural log-transformed to correct for the skewed volume distribution) instead of age. In model 2, we additionally adjusted for both white matter atrophy and WML load to identify changes to white matter microstructure, independent from the macrostructural white matter changes that may also affect the diffusivity measurements. In model 3, we added the different cardiovascular risk factors individually to model 1 to separately investigate the effect of these on change in white matter microstructure. For analyses with blood pressure and cholesterol, medication use was considered a confounder and added to the model. For the analysis of total cholesterol, HDL cholesterol was additionally included as a confounder. All global analyses were performed using SPSS (version 20).

For the localized TBSS analyses, we performed voxelwise multiple linear regressions for the same models as for the global analysis, also restricting the analyses to the (baseline) normal-appearing white matter. If significant associations were found for tests in model 3, we additionally performed an analysis correcting for measures of macrostructural white matter degeneration to rule out confounding by white matter atrophy and WML. We used threshold-free cluster enhancement[25] with default settings for skeletonized data to promote spatially clustered findings and controlled the family wise error rate by using a permutation based approach (using 5000 permutations).[27] All analyses were performed using an in-house adapted version of the Randomise tool available in FSL[25], effectively performing a voxelwise available-case analysis.

RESULTS

Table 1 shows the population characteristics of the 501 participants. Mean age at baseline MRI was 69.9 years (ranging from 64.1 to 91.1 years), and 253 (50.5%) participants were female. The global analyses, corrected for age, sex, scan interval and ICV, showed an average decrease of FA in the normal-appearing white matter skeleton of 0.0042 ($p<10^{-6}$) and an average increase of MD of 8.1 x $10^{-6}mm^2/s$ ($p<10^{-6}$) over the follow-up interval (model 1). The same changes were observed when additionally controlling for white matter atrophy and WML load (model 2). As can be seen in **Table 2**, these two additional confounding variables were also associated with changes in MD – higher WML load, less normal appearing white matter and higher age resulted in an additional increase in MD – but not with FA.

Table 1 Baseline characteristics of included participants

	N=501
Age (y)	69.9 (4.3)
Female	253 (50.5)
Follow up time (y)	2.0 (0.5)
NAWM baseline FA	0.322 (0.016)
NAWM baseline MD ($10^{-3}mm^2/s$)	0.726 (0.022)
Brain volume (mL)	1125 (114)
NAWM volume (mL)	394 (58)
WML volume (mL) †	3.74 (2.28-7.39)
Systolic blood pressure (mmHg)	142.3 (16.5)
Diastolic blood pressure (mmHg)	81.0 (9.7)
Use of blood pressure lowering medication	168 (33.7)
Diabetes mellitus	34 (6.9)
Smoking	
never	162 (32.7)
former	270 (54.4)
current	64 (12.9)
Total serum cholesterol (mmol/L)	5.73 (0.94)
Serum HDL cholesterol (mmol/L)	1.45 (0.40)
Use of lipid lowering medication	107 (21.4)
APOE-ε4 carriership	118 (23.1)

Data is presented as mean (SD) for continuous variables and number (%) for categorical variables. † White matter lesion volume presented as median (interquartile range). The following variables had missing data: cholesterol (n=3), lipid lowering medication (n=2, not overlapping with cholesterol), blood pressure (n=4), blood pressure lowering medication (n=2, overlapping with blood pressure) *APOE*-ε4 carriership (n=15), diabetes (n=5), smoking (n=5). NAWM indicates normal-appearing white matter; FA fractional anisotropy; MD mean diffusivity, WML white matter lesion.

Table 2. Demographic characteristics and global change in white matter microstructure

variable	**change in FA (x 10^{-3})**	***p* value**	**change in MD (x 10^{-6}mm^2/s)**	***p* value**
Age	*-0.12*	0.09	**0.20**	0.01
Sex	*0.37*	0.57	*-0.07*	0.93
Brain volume	*-0.18*	0.69	*0.91*	0.08
NAWM volume	*0.27*	0.51	**-1.43**	2 x 10^{-3}
ln(WML volume)	*-0.29*	0.31	**1.21**	2 x 10^{-4}

Voxelwise analyses, visualized in **Figure 1** for model 2, showed decrease in FA over the two-years follow-up interval in the majority of the brain white matter, except in most of the sensorimotor tracts. Change over time for models 1 and 2 was not materially different. Increase in FA was found in the motor tracts extending from the brain stem, through the internal capsule (both the anterior and posterior limbs) and the corona radiata up into the motor cortex (**Figure 1**). The MD increased throughout the brain, with most marked increase periventricularly and around the fornix. No voxels showed a significant decrease in MD. Amongst the voxels expressing increased FA, MD mostly increased. Constraining the voxelwise analysis to the normal-appearing white matter meant that the number of degrees-of-freedom of the analysis varied from voxel to voxel, but variation was smooth and the minimum number of subjects included per voxel for models 1 and 2 was 295.

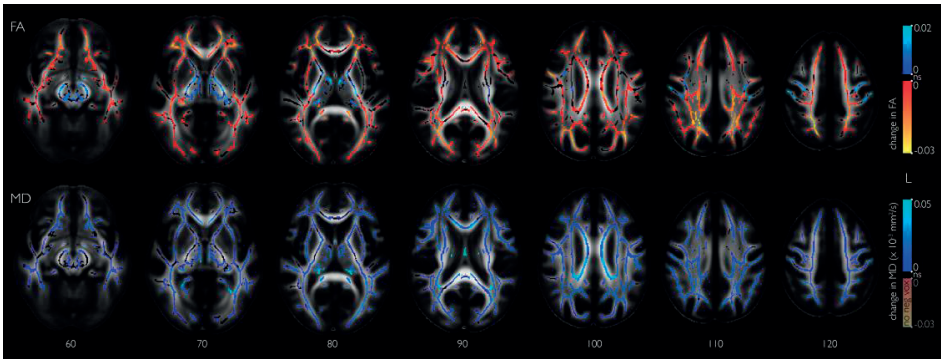

Figure 1. Change in diffusion characteristics over two-years of follow-up, corrected for age, sex, scan interval, intra cranial volume and macroscopic WM changes. The top row shows regions of significant change in fractional anisotropy (FA) over time, color coded blue to indicate increase, and red and yellow to indicate decrease in FA. The bottom row shows regions of significant change in mean diffusivity (MD), color-coded blue for increase (no voxels showed a significant decrease in MD). Results shown are $p<0.05$, the family wise error rate was controlled using a permutation approach. *P* values are presented in Supplementary Figure 2. Results are overlaid on a population specific average-FA image in MNI coordinates, showing non-significant (ns) skeleton voxels in black.

Figures 2 and 3 show how changes in FA (**Figure 2**) and MD (**Figure 3**) depended on various parameters included in models 1 and 2. For model 1, we observed associations between age and FA (decrease) or MD (increase). These associations were reduced both in strength and in extent, when additionally adding measures of macrostructural white matter changes (atrophy and WML load) in the model. The figures also show associations between white matter atrophy and WML load, and change in FA and MD in model 2 No difference in change in diffusion characteristics was observed for men and women.

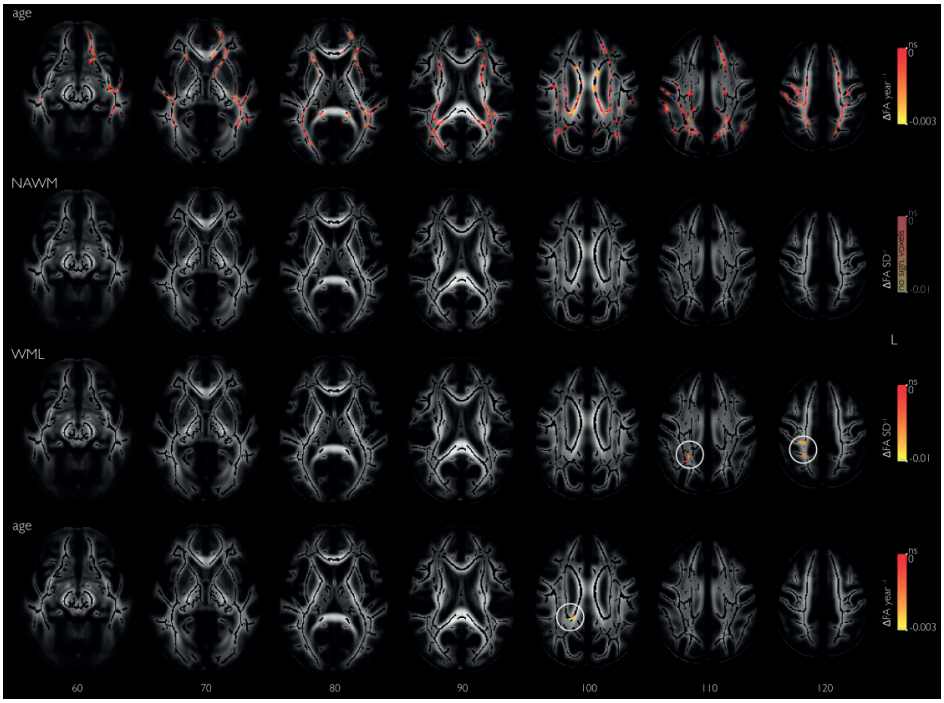

Figure 2. Age and macrostructural white matter changes at baseline and change in fractional anisotropy (FA) over two-years of follow-up. The top row shows in yellow-to-red regions of decrease in FA that relate to higher age at baseline (adjusted for sex, scan interval and intracranial volume (ICV)). The second and third row show FA changes that are associated with respectively a decrease in normal-appearing white matter (NAWM) volume and an increase in white matter lesion (WML) volume (both adjusted for age, sex, scan interval, ICV). The final row shows regions of decrease in FA related to higher age, when additionally adjusted for NAWM volume and WML volume. Inverse directions of association showed no significant voxels (not shown). Results shown are $p<0.05$, the family wise error rate was controlled using a permutation approach. *P* values are presented in Supplementary Figure 3. Results are overlaid on a population specific average-FA image in MNI coordinates, showing non-significant (ns) NAWM skeleton voxels in black.

Investigating cardiovascular risk factors in relation to longitudinal DTI changes, we only found associations for *APOE* ε4 carriership and for total serum cholesterol level. Specifically, ε4 carriers showed localized increases in FA in comparison to non-carriers, but no changes globally. These local differences were more prominent in the right than in the left hemisphere and primarily in the centrum semiovale and in the white matter adjacent to the trigone of the lateral ventricle. In contrast, we observed lower MD only in a small peritrigonal cluster in carriers compared to non-carriers. These observed associations persisted when additionally correcting for macrostructural measures of white matter degeneration. Similarly, we observed that global increase in MD to a lesser degree associated with *APOE* ε4 carriership (**Table 3**). Total serum cholesterol level was associated locally with more increase in MD in the left hemisphere. Regions included the corona radiata and white matter around the posterior and anterior horns of

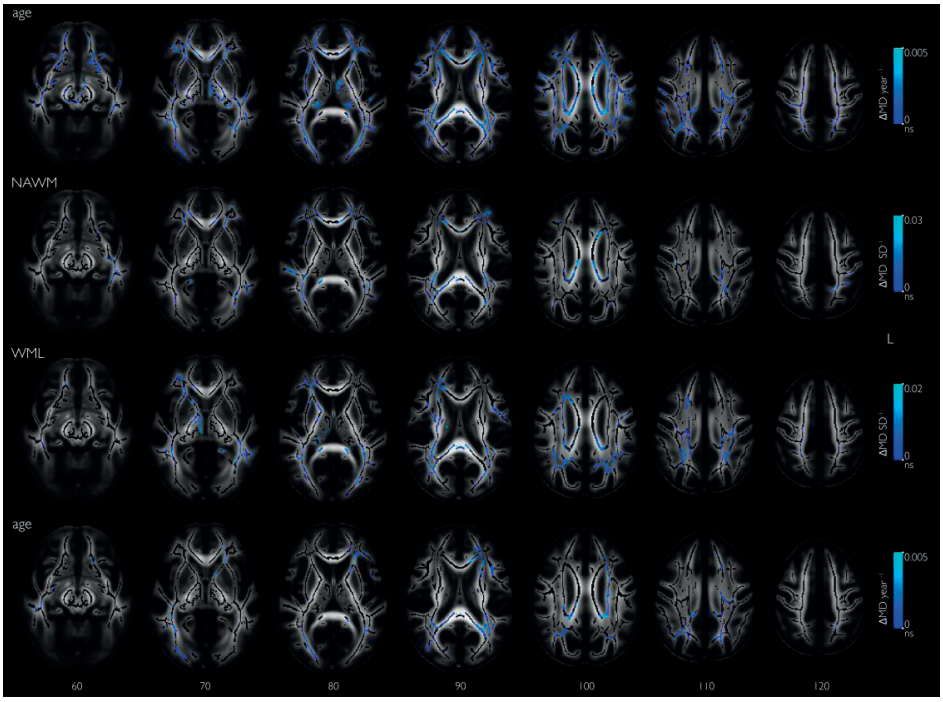

Figure 3. Age and macrostructural white matter changes at baseline and change in mean diffusivity (MD) over two-years of follow-up. The top row shows in blue regions of increase in MD that relate to higher age at baseline (adjusted for sex, scan interval and intracranial volume (ICV)). The second and third row show MD changes that are associated with respectively a decrease in normal-appearing white matter (NAWM) volume and an increase in white matter lesion (WML) volume (both adjusted for age, sex, scan interval, ICV). The final row shows regions of decrease in MD related to higher age, when additionally adjusted for NAWM volume and WML volume. Inverse directions of association showed no significant voxels (not shown). Results shown are $p<0.05$, the family wise error rate was controlled using a permutation approach. *P* values are presented in Supplementary Figure 4. Results are overlaid on a population specific average-FA image in MNI coordinates, showing non-significant (ns) NAWM skeleton voxels in black.

the lateral ventricle. These observed associations persisted when additionally correcting for macrostructural measures of white matter degeneration. Other cardiovascular risk factors were associated with neither global nor local changes in tissue microstructure. Results on global DTI characteristics are presented in **Table 3**.

Investigating cardiovascular risk factors in relation to longitudinal DTI changes, we only found associations for *APOE* ε4 carriership and for total serum cholesterol level. Specifically, ε4 carriers showed localized increases in FA in comparison to non-carriers, but no changes globally. These local differences were more prominent in the right than in the left hemisphere and primarily in the centrum semiovale and in the white matter adjacent to the trigone of the lateral ventricle. In contrast, we observed lower MD only in a small peritrigonal cluster in carriers compared to non-carriers. These observed associations persisted when additionally correcting for macrostructural measures of white matter degeneration. Similarly, we observed that global increase in MD to a lesser degree associated with *APOE* ε4 carriership (**Table 3**).

Table 3. Cardiovascular risk factors and global change in white matter microstructure

risk / protective factor	**change in FA ($\times 10^{-3}$)**	***p* value**	**change in MD ($\times 10^{-6}$mm^2/s)**	***p* value**
Systolic blood pressure	*-0.46*	0.09	*0.33*	0.29
Diastolic blood pressure	*-0.01*	0.98	*0.10*	0.76
Diabetes mellitus	*0.08*	0.77	*0.46*	0.13
Smoking (never - current)	*-0.15*	0.86	*0.22*	0.83
Total serum cholesterol	*-0.42*	0.15	*-0.09*	0.78
Serum HDL cholesterol	*0.31*	0.28	*-0.23*	0.49
APOE-ε4 carriership	*1.12*	0.07	**-1.51**	0.04

Cardiovascular risk factors and global change in white matter microstructure computed with respect to the population mean change of -0.0042 in FA ($p<10^{-6}$) and 8.1 x 10^{-6}mm^2/s in MD ($p<10^{-6}$). Values represent change in diffusion measure, per SD of change for continuous variables, or absolute for categorical variables. Significant results are shown in bold instead of italic.

Total serum cholesterol level was associated locally with more increase in MD in the left hemisphere. Regions included the corona radiata and white matter around the posterior and anterior horns of the lateral ventricle. These observed associations persisted when additionally correcting for macrostructural measures of white matter degeneration. Other cardiovascular risk factors were associated with neither global nor local changes in tissue microstructure. Results on global DTI characteristics are presented in **Table 3**.

DISCUSSION

In this large, population-based longitudinal sample of elderly persons, we found changes to microstructural tissue organization congruent with microstructural white matter deterioration. Over a two-year follow-up interval, loss of microstructure was globally reflected in decreases in FA and increases in MD, independent of severity of white matter atrophy and WML load. On a voxelwise level, we found regional differences in white matter changes, with decreased FA in most of the brain, but increased FA in most of the sensorimotor pathway, running from the brainstem up to the motor cortex. In contrast, MD was increased throughout the white matter skeleton, without any significant decreases. We found that white matter deterioration was locally more pronounced with higher age, indicating that older persons show more change in white matter microstructure over the same follow-up time than younger persons. This could partly be explained by macroscopic measures of white matter degeneration, i.e. white matter atrophy and WML load, which also increase with age. We only identified few associations between known (cardiovascular) determinants of white matter atrophy and WML load and changes in diffusion characteristics over time, both globally and locally. These findings contribute to our understanding of age related brain changes, and thereby may aid in the future identification of early pathology leading to disease.

Cross-sectional studies of normal aging of white matter have generally shown lower FA and higher MD with higher age[1,11,12] which is in line with our results. In a cross-sectional analysis of an earlier time point for the same population we found a similar effect with age itself, i.e. most of the associations with age were driven by macroscopic measures of white matter degeneration.[10] Both results indicate that white matter degeneration with aging is not intrinsically due to aging alone nor purely driven by macroscopic measures of white matter degeneration. Longitudinal analyses, which are necessary to reliably characterize change over time, have found reductions in FA and increases in MD.[6,9] Our findings confirm much of these longitudinal and cross sectional findings, and extend on these for the normal appearing white matter, in a larger population.

In the *sensorimotor* pathway, we identified a seemingly paradoxical increase of FA, which may relate to partial volume mixing of multiple fiber tracts (e.g. crossing or touching fibers) within these voxels. Selective degeneration of one fiber bundle with relative sparing of the other bundle may lead to an increase in FA, with concomitant increase in MD. This effect was previously observed in a study on Wallerian degeneration[28], and described in detail in a cross-sectional study on Alzheimer's disease.[29] The increased FA, ascending from the brain stem, through the internal capsule and the corona radiata up into the motor cortex – regions with either crossing fibers or closely spaced adjacent fibers[30-31] – thereby seems to indicate a relative sparing of sensorimotor fibers. Inside the *fornix* we found the strongest increase in MD. This may reflect

loss of microstructural organization in this limbic fiber, but we should note that this tract is small compared to our imaging matrix and surrounded by CSF. These findings therefore likely represent a combination of microstructural and macrostructural (i.e. tract thinning) changes.[32]

We did observe counter-intuitive associations with *APOE* ε4 carriership. Globally we observed a decrease in MD in carriers compared to non-carriers. Locally, we observed in *APOE* ε4 carriers increases in FA in comparison to non-carriers, in regions with a high prevalence of WML. These observations are in contrast to cross-sectional studies with *APOE* genotype, which have generally shown widespread deterioration of white matter microstructure associated with the ε4 allele.[33,34] On closer inspection this paradoxical increase in FA was largely explained by lower baseline FA for carriers, and a larger decrease in FA for non-carriers. Higher serum cholesterol was associated to stronger increases in MD over time in the left hemisphere. When investigating other cardiovascular risk factors, we observed associations with neither global nor local changes to white matter microstructure, which is in line with another longitudinal study[6] but in disagreement to cross-sectional observations.[2,35] These discrepancies, both for *APOE* and cardiovascular factors, might be due to the relatively short follow-up interval, which translates in the (clustered) voxelwise and global statistics being relatively underpowered. Another possibility is that changes induced by cardiovascular risk factors may be more prominent in the periphery of white matter tracts, whereas the TBSS method we used focused on tract centers. Most importantly however, our longitudinal design only probes differential effects, and not the difference accumulated over the total exposure time, which precludes the analysis from finding subtle differential changes with cardiovascular risk factors.

Limitations of our study are: 1. The relatively short follow-up interval, which may have limited the sensitivity to detect differences over time. Especially in the case of differential effects with risk factors (as mentioned above), this meant we could not disambiguate the risk factor-related changes from the large changes associated with aging. This also impedes direct translation of our findings to individual subjects, e.g. for use in clinical care. 2. The study protocol was defined in 2005-2006 and therefore the spatial resolution for the diffusion acquisition was relatively poor for current day standards.[23] Although the use of TBSS mitigates partial volume effects in the major white matter tracts and we adjusted for overall white matter atrophy, we will have been less sensitive to detect change in very thin tracts. We did nevertheless identify widespread deterioration of white matter microstructure within the studied interval. We excluded participants with dementia at either time point, but we did not exclude persons with mild cognitive impairment (MCI), since MCI contributes to the continuous spectrum of age related pathologies that we aim to investigate. This may have led

to inclusion of some persons with preclinical dementia, which could have affected our results.

In conclusion, in this large longitudinal analysis of brain white matter microstructure in normal aging, we found widespread microstructural deterioration of the normal-appearing white matter, with relative sparing of sensorimotor fibers**.** We found changes to be more prominent in older persons, which were partly explained by concomitant macroscopic white matter pathology. Cardiovascular risk factors did not generally relate to white matter microstructure. These insights into white matter degeneration in aging may help in understanding the pathophysiology of neurodegenerative diseases.

CHAPTER REFERENCES

1. Sullivan E V., Pfefferbaum A. Diffusion tensor imaging and aging. Neurosci Biobehav Rev. 2006;30(6):749–61.
2. Gons RAR, van Oudheusden LJB, de Laat KF, van Norden AGW, van Uden IWM, Norris DG, et al. Hypertension is related to the microstructure of the corpus callosum: the RUN DMC study. J. Alzheimers. Dis. 2012 Jan;32(3):623–31.
3. Beaulieu C. The basis of anisotropic water diffusion in the nervous system - a technical review. NMR Biomed. 2002;15(7-8):435–55.
4. O'Sullivan M, Jones DK, Summers PE, Morris RG, Williams SC, Markus HS. Evidence for cortical "disconnection" as a mechanism of age-related cognitive decline. Neurology. 2001 Aug;57(4):632–8.
5. Oishi K, Mielke MM, Albert M, Lyketsos CG, Mori S. DTI analyses and clinical applications in Alzheimer's disease. J. Alzheimers. Dis. 2011 Jan;26 Suppl 3:287–96.
6. Barrick TR, Charlton RA, Clark CA, Markus HS. White matter structural decline in normal ageing; a prospective longitudinal study using tract based spatial statistics. Neuroimage. 2010 Jun;51(2):565–77.
7. Teipel SJ, Meindl T, Wagner M, Stieltjes B, Reuter S, Hauenstein K-H, et al. Longitudinal changes in fiber tract integrity in healthy aging and mild cognitive impairment: a DTI follow-up study. J. Alzheimers. Dis. 2010 Jan;22(2):507–22.
8. Sullivan E V., Rohlfing T, Pfefferbaum A. Longitudinal study of callosal microstructure in the normal adult aging brain using quantitative DTI fiber tracking. Dev. Neuropsychol. 2010 Jan;35(3):233–56.
9. Sexton CE, Walhovd KB, Storsve AB, Tamnes CK, Westlye LT, Johansen-Berg H, et al. Accelerated Changes in White Matter Microstructure during Aging: A Longitudinal Diffusion Tensor Imaging Study. J. Neurosci. 2014 Nov 12;34(46):15425–36.
10. Vernooij MW, de Groot M, van der Lugt A, Ikram MA, Krestin GP, Hofman A, et al. White matter atrophy and lesion formation explain the loss of structural integrity of white matter in aging. Neuroimage. 2008 Nov;43(3):470–7.
11. Abe O, Aoki S, Hayashi N, Yamada H, Kunimatsu A, Mori H, et al. Normal aging in the central nervous system: quantitative MR diffusion-tensor analysis. Neurobiol Aging. 2002;23(3):433–41.
12. Burzynska AZ, Preuschhof C, Bäckman L, Nyberg L, Li S-C, Lindenberger U, et al. Age-related differences in white matter microstructure: region-specific patterns of diffusivity. Neuroimage. Elsevier Inc.; 2010 Feb 1;49(3):2104–12.
13. Nusbaum AO, Tang CY, Buchsbaum MS, Wei TC, Atlas SW. Regional and global changes in cerebral diffusion with normal aging. AJNR. Am. J. Neuroradiol. 2001 Jan;22(1):136–42.
14. Lee DY, Fletcher E, Martinez O, Zozulya N, Kim J, Tran J, et al. Vascular and degenerative processes differentially affect regional interhemispheric connections in normal aging, mild cognitive impairment, and Alzheimer disease. Stroke. 2010 Aug;41(8):1791–7.
15. Groot M De, Ikram MA, Akoudad S, Krestin GP, de Groot M, Ikram MA, et al. Tract-specific white matter degeneration in aging . The Rotterdam Study. Alzheimer's Dement. Elsevier Ltd; 2014 Sep 9;11(3):1–10.
16. Hofman A, Darwish Murad S, van Duijn CM, Franco OH, Goedegebure A, Ikram MA, et al. The Rotterdam Study: 2014 objectives and design update. Eur. J. Epidemiol. 2013 Nov;28(11):889–926.
17. Ikram MA, van der Lugt A, Niessen WJ, Krestin GP, Koudstaal PJ, Hofman A, et al. The Rotterdam Scan Study: design and update up to 2012. Eur. J. Epidemiol. 2011 Oct 16;26(10):811–24.

18. Vrooman HA, Cocosco CA, van der Lijn F, Stokking R, Ikram MA, Vernooij MW, et al. Multi-spectral brain tissue segmentation using automatically trained k-Nearest-Neighbor classification. Neuroimage. 2007 Aug;37(1):71–81.
19. De Boer R, Vrooman HA, van der Lijn F, Vernooij MW, Ikram MA, van der Lugt A, et al. White matter lesion extension to automatic brain tissue segmentation on MRI. Neuroimage. Elsevier Inc.; 2009 May 1;45(4):1151–61.
20. Greve DN, Fischl B. Accurate and robust brain image alignment using boundary-based registration. Neuroimage. Elsevier Inc.; 2009 Oct 15;48(1):63–72.
21. Koppelmans V, de Groot M, de Ruiter MB, Boogerd W, Seynaeve C, Vernooij MW, et al. Global and focal white matter integrity in breast cancer survivors 20 years after adjuvant chemotherapy. Hum. Brain Mapp. 2014 Dec 20;35(3):889–99.
22. Leemans A, Jeurissen B, Sijbers J, Jones DK. ExploreDTI: a graphical toolbox for processing, analyzing, and visualizing diffusion MR data. Proc. 17th Sci. Meet. Int. Soc. Magn. Reson. Med. 2009. p. 3537.
23. De Groot M, Vernooij MW, Klein S, Ikram MA, Vos FM, Smith SM, et al. Improving alignment in Tract-based spatial statistics: evaluation and optimization of image registration. Neuroimage. 2013 Aug 1;76:400–11.
24. Smith SM, Jenkinson M, Johansen-Berg H, Rueckert D, Nichols TE, Mackay CE, et al. Tract-based spatial statistics: voxelwise analysis of multi-subject diffusion data. Neuroimage. 2006 Jul;31(4):1487–505.
25. Jenkinson M, Beckmann CF, Behrens TEJ, Woolrich MW, Smith SM. FSL. Neuroimage. 2012 Aug 15;62(2):782–90.
26. Smith SM, Nichols TE. Threshold-free cluster enhancement: addressing problems of smoothing, threshold dependence and localisation in cluster inference. Neuroimage. 2009 Jan;44(1):83–98.
27. Nichols TE, Holmes AP. Nonparametric permutation tests for functional neuroimaging: a primer with examples. Hum Brain Mapp. 2002 Jan;15(1):1–25.
28. Pierpaoli C, Barnett A, Pajevic S, Chen R, Penix LR, Virta A, et al. Water diffusion changes in Wallerian degeneration and their dependence on white matter architecture. Neuroimage. 2001 Jun;13(6 Pt 1):1174–85.
29. Douaud G, Jbabdi S, Behrens TEJ, Menke RA, Gass A, Monsch AU, et al. DTI measures in crossing-fibre areas: increased diffusion anisotropy reveals early white matter alteration in MCI and mild Alzheimer's disease. Neuroimage. 2011 Apr 1;55(3):880–90.
30. Jeurissen B, Leemans A, Tournier J-D, Jones DK, Sijbers J. Investigating the prevalence of complex fiber configurations in white matter tissue with diffusion magnetic resonance imaging. Hum. Brain Mapp. 2013 Nov;34(11):2747–66.
31. Oishi K, Faria A V., Zijl PCM van, Mori S. MRI Atlas of Human White Matter, Second Edition. Academic Press; 2010.
32. Berlot R, Metzler-Baddeley C, Jones DK, O'Sullivan MJ. CSF contamination contributes to apparent microstructural alterations in mild cognitive impairment. Neuroimage. The Authors; 2014 Mar 3;92C:27–35.
33. Persson J, Lind J, Larsson A, Ingvar M, Cruts M, Van Broeckhoven C, et al. Altered brain white matter integrity in healthy carriers of the APOE epsilon4 allele: a risk for AD? Neurology. 2006 Apr 11;66(7):1029–33.
34. Westlye LT, Reinvang I, Rootwelt H, Espeseth T. Effects of APOE on brain white matter microstructure in healthy adults. Neurology. 2012 Nov 6;79(19):1961–9.

35. Salat DH, Williams VJ, Leritz EC, Schnyer DM, Rudolph JL, Lipsitz LA, et al. Inter-individual variation in blood pressure is associated with regional white matter integrity in generally healthy older adults. Neuroimage. Elsevier B.V.; 2012 Jan 2;59(1):181–92.